BILINGUAL PUBLISHING GROUP

Research in Ecology

https://journals.bilpubgroup.com/index.php/re

ARTICLE

Use of Remote Sensing for Multitemporal Analysis of the Severity of the Fontibón Fire in Pamplona, Colombia

Carlos E. Oliveros-Valero [1,2], Javier Yesid Villamizar Vera [1,3], William Vera Arias[2], Sergio Daniel Parada [2], Klaus Faber Mogollon [4], Antonio Manuel Jr. Collazos Gámez [2], Vladimir Henao-Céspedes [1], Yeison Alberto Garcés-Gómez [1*]

[1] *Faculty of Engineering and Architecture, Universidad Católica de Manizales, Manizales 170001, Colombia; carlos.oliveros@ucm.edu.co (C.E.O.-V.); javier.villamizar@ucm.edu.co (J.Y.V.V.); vhenao@ucm.edu.co (V.H.-C.)*

[2] *Secretaría Departamental, Gestión del Riesgo de Norte de Santander, Bucaramanga 680006, Colombia; warias@sdgr.gov.co (W.V.A.); sparada@sdgr.gov.co (S.D.P.); ajrcollazos@sdgr.gov.co (A.M.J.C.G.)*

[3] *Instituto Geográfico Agustín Codazzi-IGAC, Bogotá 111061, Colombia*

[4] *Alcaldía de Pamplona, Pamplona 543050, Colombia; kfmogollon@pamplona.gov.co*

ABSTRACT

Wildfires in tropical mountain ecosystems are difficult to assess because steep terrain and persistent cloud cover constrain field surveys and satellite observation. This study developed an integrated workflow combining Unmanned Aerial Vehicle (UAV) photogrammetry, Sentinel-2 imagery, and Google Earth Engine to quantify burn severity and early vegetation recovery after the January 2024 Fontibón fire in Pamplona, Colombia. RGB imagery acquired with a DJI Mavic 3E was processed in Agisoft Metashape to delineate the affected area and produce 3-cm orthophotos. Sentinel-2 Normalized Burn Ratio (NBR) and differenced Normalized Burn Ratio (dNBR) were used to classify severity, while Normalized Difference Vegetation Index (NDVI) images from January 2024 and January 2026 characterized greenness trajectories. UAV orthophotos supported image-based validation through 500 purely random checkpoints. The fire affected 175 ha, of which 61.9% showed moderate-high or high severity. Classification agreement with UAV visual interpretation was 87.4% (Cohen's $\kappa = 0.82$). Mean NDVI declined from 0.62 ± 0.09 before the fire to 0.28 ± 0.13 immediately afterward and

*CORRESPONDING AUTHOR:
Yeison Alberto Garcés-Gómez, Faculty of Engineering and Architecture, Universidad Católica de Manizales, Manizales 170001, Colombia; Email: ygarces@ucm.edu.co

ARTICLE INFO
Received: 27 May 2026 | Revised: 28 July 2026 | Accepted: 5 August 2026 | Published Online: 24 August 2026
DOI: https://doi.org/10.30564/re.v8i4.13568

CITATION
Oliveros-Valero, C.E., Villamizar Vera, J.Y., Vera Arias, W., et al., 2026. Use of Remote Sensing for Multitemporal Analysis of the Severity of the Fontibón Fire in Pamplona, Colombia. Research in Ecology. 8(4): 327–338. DOI: https://doi.org/10.30564/re.v8i4.13568

increased to 0.38 ± 0.06 by 2026 (paired *t*-test, $p < 0.001$). Although 98.7% of the area showed moderate greenness by 2026, no zone returned to the pre-fire high-NDVI class. These results indicate widespread spectral greening without evidence of complete structural or ecological recovery. The workflow provides operational inputs for restoration planning, but UAV image interpretation is not independent ecological ground truth, the validation sample was not stratified by severity, and the two-year observation window limits long-term ecological inference.
Keywords: Sentinel-2; Burn Severity; Vegetation Recovery; dNBR; UAV; Colombian Andes

1. Introduction

Wildfires are a major global threat with ecological, socioeconomic, and climatic consequences. They can reduce biodiversity and habitat complexity, particularly in fire-sensitive ecosystems [1]. Fires also degrade soils by increasing hydrophobicity and reducing surface organic carbon [2,3]. In addition, they release greenhouse gases that reinforce climate warming and threaten nearby communities [4]. The resulting social and economic burdens are especially severe for rural populations [5].

Tropical mountain regions such as Fontibón, in Pamplona (Norte de Santander, Colombia), combine several factors that increase wildfire risk. ENSO-related climate variability promotes drought [6], while steep slopes can accelerate fire spread [1]. Anthropogenic ignition and landscape transformation are also central components of fire dynamics in the northern Andes [7]. This context underscores the need for methods that can quantify fire impacts and support adaptive restoration.

Conventional post-fire assessments rely on *in situ* inspections and vegetation inventories. Although these methods provide detailed local information, they are expensive, spatially limited, and difficult to implement in rugged or unsafe terrain [8]. Field-based severity assessment can also vary among observers and may sample only a small fraction of a burned area [9]. Remote sensing therefore provides a scalable complement for mapping disturbance and monitoring recovery [10,11]. It does not, however, replace ecological field measurements.

Geospatial technologies provide complementary observation scales. Sentinel-2 offers frequent, open-access multispectral coverage, while UAV imagery provides sub-decimetric detail for localized assessment [12,13]. The Normalized Burn Ratio (NBR) uses near-infrared and short-wave infrared reflectance to detect fire-related surface change [14]. The differenced Normalized Burn Ratio (dNBR) compares pre- and post-fire NBR, whereas the relativized dNBR (RdNBR) accounts for differences in pre-fire vegetation density [15,16]. Recent UAV studies further demonstrate the value of high-resolution RGB and multispectral imagery for classifying burned areas and severity [17].

Combining satellite and UAV products can link broad spatial coverage with local detail, but cross-scale comparison should not be confused with complete quantitative data fusion. GIS-based severity products can nevertheless support restoration prioritization and risk-management decisions [18,19]. Recent studies have examined fire precursors and post-fire mapping in tropical and subtropical settings, including Colombia, Ecuador, and Yunnan [20–22]. Machine-learning and object-based approaches also provide promising routes for integrating multisource imagery [23–25], while NPP-based analysis can extend interpretation beyond greenness alone [26].

This study develops and applies an integrated remote-sensing workflow to evaluate the Fontibón wildfire and support post-fire management. The objectives were to: (1) delineate the affected area using RGB UAV photogrammetry and 3D processing; (2) classify burn severity from Sentinel-2 dNBR using established thresholds; and (3) generate spatial evidence for restoration prioritization. The contribution lies in combining UAV-derived spatial detail, Sentinel-2 severity mapping, and two-year NDVI monitoring in a tropical mountain setting with persistent cloud cover and limited field access. Throughout this study, dNBR denotes the differenced Normalized Burn Ratio.

2. Materials and Methods

2.1. Study Area

Pamplona is located in Norte de Santander, northeastern Colombia (**Figure 1**), in the Eastern Cordillera of the Andes. The municipality lies at approximately 2,342 m a.s.l. and has a cool mountain climate, with typical temperatures of 10–18 °C. The landscape is characterized by steep terrain and recurrent low-level fog.

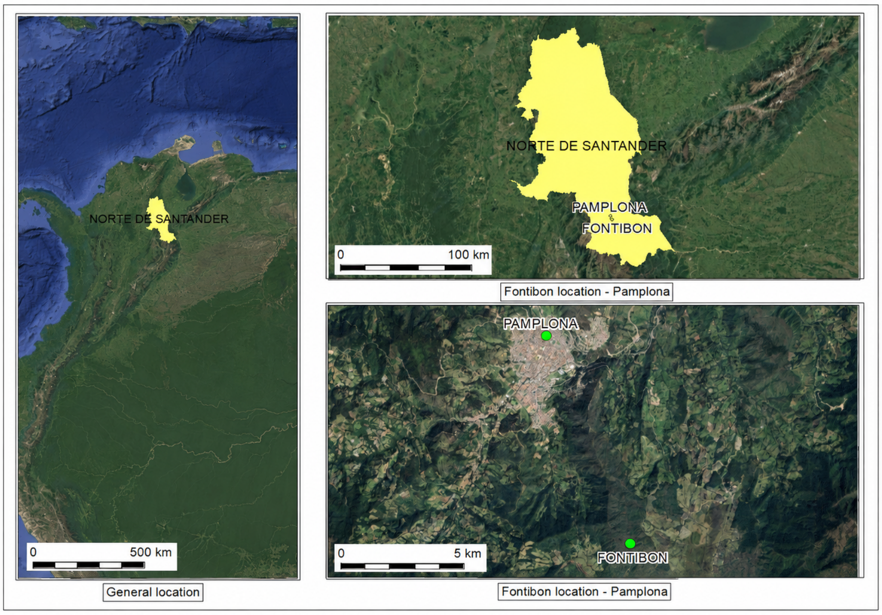

Figure 1. Geographical location of the Fontibón study area, Pamplona, Norte de Santander, Colombia.

2.2. UAV Photogrammetry and Image Acquisition via Google Earth Engine

UAV imagery was acquired after a pre-flight risk assessment, coordination with local airspace activities, and identification of no-fly zones. DJI Pilot was used to configure the flight plan. The mission targeted a ground sampling distance of ≤3 cm/pixel, with 80% forward overlap and 70% side overlap. A DJI Mavic 3E equipped with a 20 MP RGB camera, 4/3-inch CMOS sensor, and mechanical shutter was used. Autonomous flight lines were supplemented with manual inspections of critical areas. Photogrammetric processing was performed in Agisoft Metashape Professional (Agisoft LLC, St. Petersburg, Russia). The workflow included image alignment, dense point-cloud generation, surface reconstruction, digital surface model generation, and orthomosaic export.

The pre-fire baseline corresponded to 5 January 2024. The immediate post-fire image was acquired on 25 January 2024, after smoke had dissipated but before substantial herbaceous regrowth. Recovery was assessed on 5 January 2026 to maintain comparable seasonal timing.

Google Earth Engine supports reproducible multi-temporal classification workflows [27]. Sentinel-2 surface-reflectance images were filtered by date and study-area intersection. Clouds and cloud shadows were masked using the QA60 quality band, and median composites were generated for the pre-fire, post-fire, and recovery periods. Each composite was then clipped to the study-area boundary.

2.3. Wildfire Detection and Burn Severity Assessment

The Normalized Burn Ratio (NBR) was calculated from Sentinel-2 Band 8A (narrow NIR, 865 nm) and Band 12 (SWIR, 2202 nm). This combination is sensitive to fire-related changes in vegetation water content, ash, charcoal, and exposed soil [28]. NBR was calculated as shown in Equation (1):

$$NBR = \frac{(NIR\ -\ SWIR)}{(NIR\ +\ SWIR)} \tag{1}$$

NBR ranges from −1 to 1. High values generally indicate dense, moist vegetation, whereas burned surfaces commonly show reduced NIR reflectance and increased SWIR reflectance because of foliage loss, charcoal, ash, and soil exposure [29].

Burn-related spectral change was estimated with the differenced Normalized Burn Ratio (dNBR), calculated by subtracting post-fire NBR from pre-fire NBR (Equation (2)):

$$dNBR{=}NBR_{pre-fire}{-}NBR_{post-fire} \tag{2}$$

$NBR_{pre\text{-}fire}$ represents the pre-event vegetation and moisture baseline, and $NBR_{post\text{-}fire}$ represents the post-event condition. Larger positive *dNBR* values indicate greater spectral change associated with burning. Severity classes followed the framework of Key and Benson[15] (**Table 1**). These classes describe remotely sensed burn effects and should not be interpreted as direct measurements of ecological function.

Table 1. Burn Severity Classification.

Burn Severity Level	dNBR Threshold	Interpretation and Evidences	Ecological Impact
High Severity	>0.66	Strong spectral and visible surface change, extensive canopy consumption, ash, and soil exposure.	Potential loss of biological legacies and elevated erosion risk; ecosystem-function effects were not measured.
Moderate-High Severity	0.44–0.66	Marked canopy consumption and soil exposure with some structural elements retained.	Recovery may depend on surviving vegetation and propagules; species responses were not measured.
Moderate-Low Severity	0.27–0.44	Partial surface burning with substantial vegetation cover retained.	Natural recovery may be possible, but recovery time and soil response require field confirmation.
Low Severity	0.1–0.27	Limited spectral change consistent with effects on fine fuels and minor charring.	Potentially rapid greenness recovery; biodiversity effects were not evaluated.
Unburned Area	0 ± 0.1	No detectable fire-related spectral change at Sentinel-2 scale.	Possible local refuge; ecological condition and function require field verification.

On-site verification was not possible because of rugged terrain and post-fire safety restrictions. Accordingly, 500 purely random—not severity-stratified—checkpoints were overlaid on the dNBR map. At each checkpoint, the assigned dNBR class was compared with visual interpretation of the 3-cm UAV orthophoto using vegetation consumption, soil exposure, and charcoal presence as image-based indicators. Overall agreement was 87.4% (Cohen's $\kappa = 0.82$; $p < 0.001$). Because this design was not stratified, uncommon severity classes may be underrepresented. Moreover, UAV image interpretation is a high-resolution visual reference, not independent ecological ground truth.

3. Results

The workflow delineated a 175-ha fire-affected area located approximately 1.1 km from the urban center of Pamplona (**Figure 2**). UAV orthophotos and 3D products captured patch-scale variation, while Sentinel-2 composites provided the spatial distribution of pre-fire NBR, post-fire NBR, and dNBR (**Figure 3**).

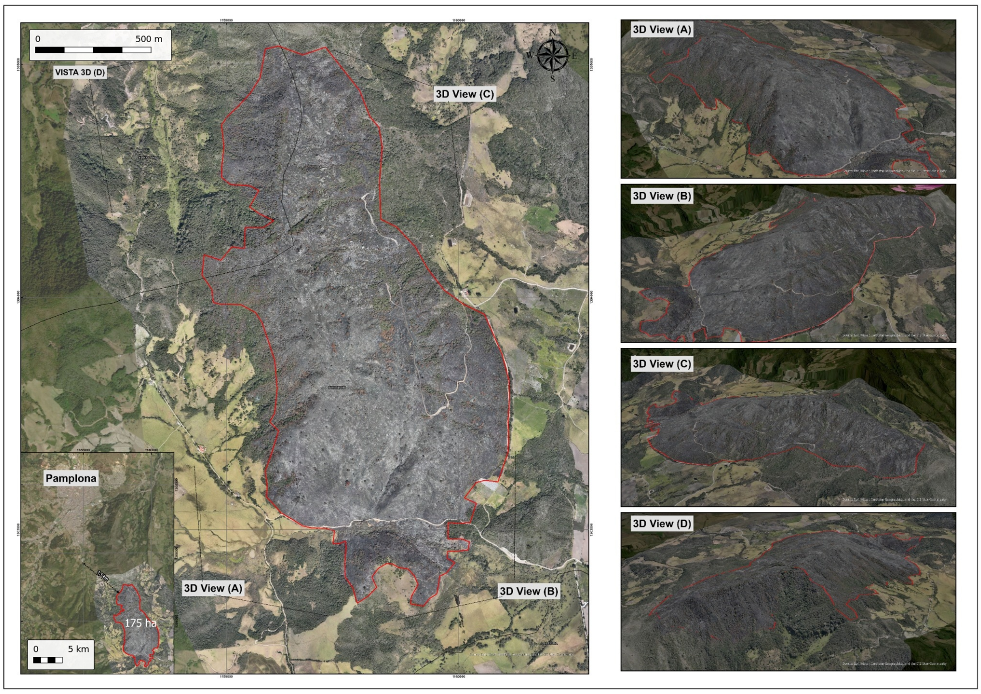

Figure 2. Delineation of the fire core using UAV-derived 3D photogrammetric models. Area A Orthophoto mosaic (GSD = 3 cm/pixel) of the 175 ha burned area; Area B Digital Surface Model (DSM) showing elevation range (2,200–2,600 m a.s.l.) and steep slopes (>30° in red); Area C Fire perimeter (yellow line) overlaid on pre-fire RGB imagery; Area D 3D perspective view (vertical exaggeration × 2) showing the proximity to Pamplona urban area (visible in upper right).

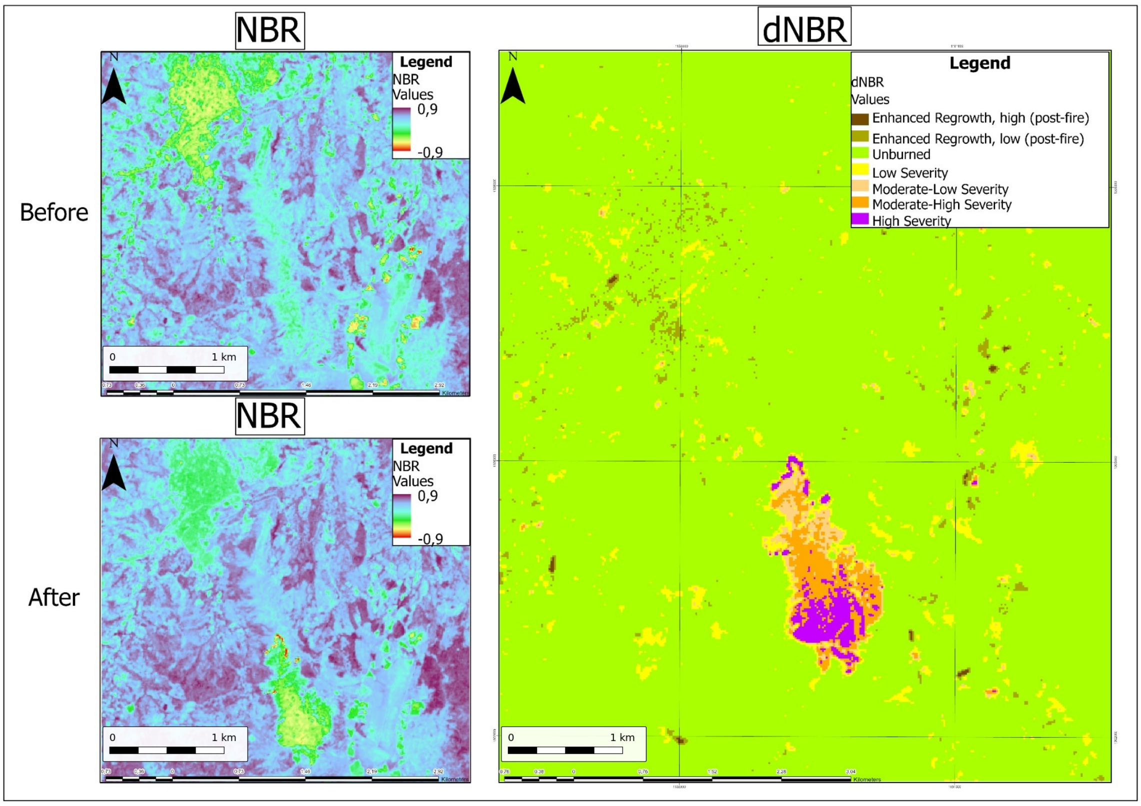

Figure 3. Pre-fire NBR, post-fire NBR, and dNBR severity. Pre-fire image: 5 January 2024; post-fire image: 25 January 2024. In the dNBR map, red indicates high severity (>0.66), orange moderate-high (0.44–0.66), yellow moderate-low (0.27–0.44), light green low (0.10–0.27), and dark green unburned (0 ± 0.1).

Moderate-high severity (0.44–0.66) covered 62.55 ha, and high severity (>0.66) covered 45.56 ha. Together, these classes accounted for 61.9% of the mapped area. Moderate-low severity (0.27–0.44) covered 32.54 ha, low severity (0.10–0.27) covered 21.68 ha, and 12.32 ha were mapped as unburned (**Table 2**).

Table 2. dNBR Interpretation.

Burn Severity Level	dNBR Range	Area (ha)	Percentage (%)	Technical Explanation
Enhanced Regrowth	−0.50 to −0.10	0.00	0.00	No areas with post-fire vegetative growth were detected.
Low Regrowth	−0.10 to 0.00	0.00	0.00	No areas with post-fire vegetative growth were detected.
Unburned	0.00 to 0.10	12.32	7.05	Evidence of baseline areas that did not experience fire degradation.
Low Severity	0.10 to 0.27	21.68	12.42	Vegetation within this range exhibited minor canopy or surface alteration.
Moderate-Low Severity	0.27 to 0.44	32.54	18.63	Vegetation within this range showed partial burning of structural layers.
Moderate-High Severity	0.44 to 0.66	62.55	35.81	Vegetation within this range displayed significant scorched and burned patches.
High Severity	>0.66	45.56	26.10	Severe vegetative destruction resulting in total canopy loss and bare soil exposure.

For sensitivity analysis, RdNBR and RBR were calculated for a stratified random sample of 1,000 pixels. The correlation between dNBR and RdNBR was r = 0.94 ($p < 0.001$), corresponding to $R^2 = 0.88$, and severity-class agreement was 91.2% (see **Figure 4** and **Table 3**).

The dNBR-RdNBR in **Table 3** comparison showed a strong linear relationship (**Figure 5**). The dNBR-RBR pattern was nonlinear (**Figure 6**), as expected from ratio normalization; therefore, fitting and reporting a simple linear equation for **Figure 6** would be misleading.

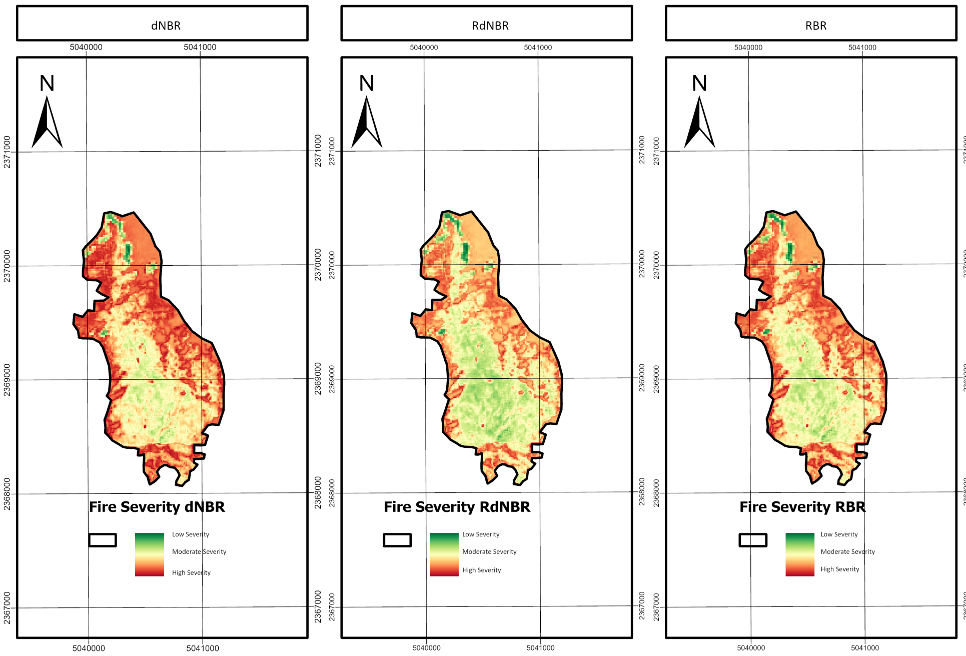

Figure 4. Comparative severity maps derived from dNBR, RdNBR, and RBR. Colors indicate low (green), medium (yellow), and high (red) severity.

Table 3. Areas by severity class derived from dNBR, RdNBR, and RBR.

Index	Class	Area_Ha	Percentage
dNBR	High Regrowth	0.00	0.0
dNBR	Low Regrowth	0.00	0.0
dNBR	Unburned	12.33	7.1
dNBR	Low Severity	21.71	12.4
dNBR	Medium – low severity	32.57	18.6
dNBR	Medium – high severity	62.62	35.8
dNBR	High severity	45.60	26.1
RdNBR	High Regrowth	0.00	0.0
RdNBR	Low Regrowth	0.00	0.0
RdNBR	Unburned	14.78	8.5
RdNBR	Low Severity	25.55	14.6
RdNBR	Medium – low severity	45.12	25.8
RdNBR	Medium – high severity	80.49	46.0
RdNBR	High Severity	8.89	5.1
RBR	High Regrowth	0.00	0.0
RBR	Low Regrowth	0.00	0.0
RBR	Unburned	16.86	9.6
RBR	Low Severity	35.54	20.3
RBR	Medium – low severity	51.01	29.2
RBR	Medium – high severity	70.42	40.3
RBR	High Severity	1.00	0.6

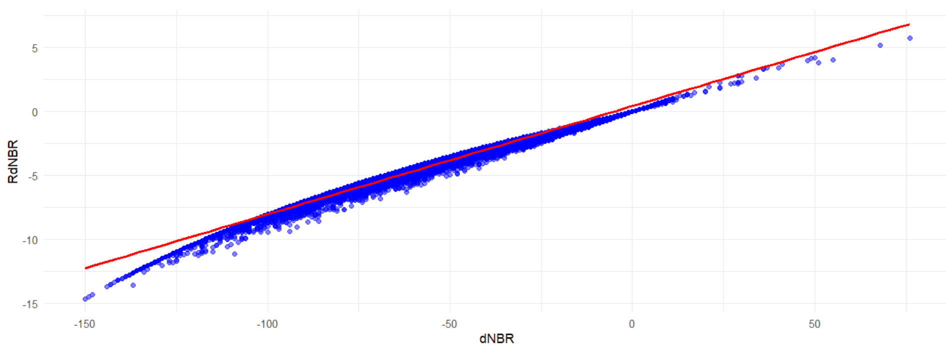

Figure 5. Scatter plot of dNBR vs. RdNBR for the stratified sample. Linear fit using the plotted scaled values: RdNBR = 0.0845 × dNBR + 0.419; R^2 = 0.88; n = 1,000; $p < 0.001$.

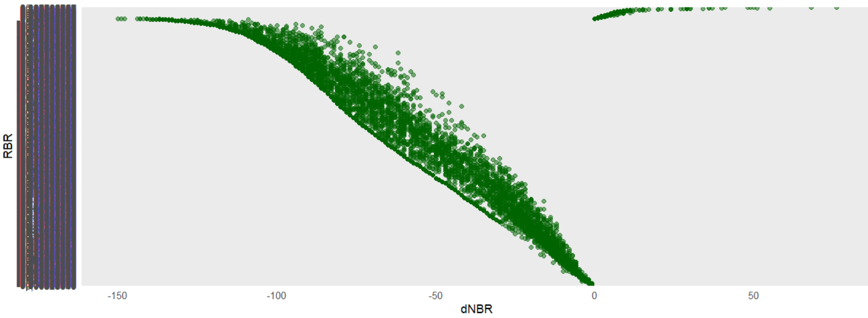

Figure 6. Scatter plot of dNBR vs. RBR (n = 1,000). The relationship is nonlinear; therefore, a linear equation and R^2 are not reported.

Quantitative comparison showed: (i) a negative association between dNBR and UAV-derived canopy surface height (Spearman's $\rho = -0.87$; $p < 0.001$); (ii) 87.4% agreement between dNBR classes and UAV visual interpretation; and (iii) 12.3 ha of unburned refugia visible in UAV orthophotos but partly mixed within 10-m Sentinel-2 pixels. Sentinel-2 classified 7.05% of the area as unburned, compared with 8.9% from UAV interpretation.

To evaluate vegetation recovery within the affected area, the Normalized Difference Vegetation Index (NDVI) was analyzed by comparing pre- and post-fire conditions calculated using Equation (3):

$$\mathrm{NDVI} = \frac{\mathrm{NIR} - \mathrm{RED}}{\mathrm{NIR} + \mathrm{RED}} \tag{3}$$

Where:

- NIR is the amount of near-infrared light reflected by the surface (Sentinel-2 Band 8).
- RED is the surface reflectance in the visible red band (Sentinel-2 Band 4) [30].

The NDVI series represented three periods: pre-fire (5 January 2024), immediate post-fire (25 January 2024), and recovery (5 January 2026). Before the fire, 95.1% of the area was in the high NDVI class (>0.5). Immediately after the fire, 54.2% was in the low class (≤0.2) and 31.4% in the moderate class (0.2–0.5). By 2026, 98.7% was in the moderate class and 1.3% remained in the low class; no area returned to the high class. Spatial patterns are shown in **Figures 7** and **8**, and area summaries are reported in **Tables 4** and **5**.

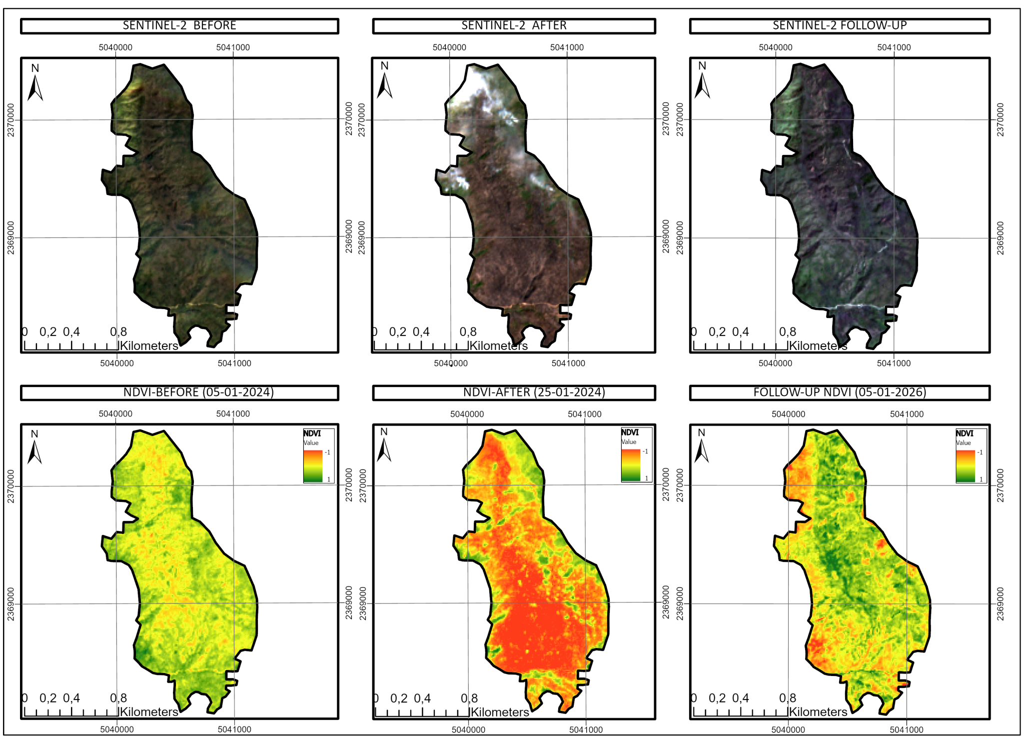

Figure 7. Multitemporal NDVI trajectories (January 2024 pre-fire, January 2024 post-fire, January 2026 recovery). Bottom left NDVI: 95.1% of area > 0.5 (dark green); Bottom center Post-fire NDVI: 54.2% ≤ 0.2 (red/brown); Bottom right Recovery NDVI: 98.7% in moderate class (0.2–0.5, light green).

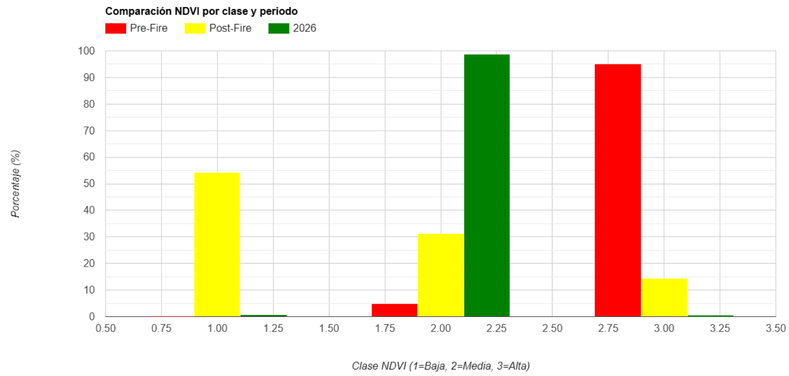

Figure 8. Comparison of NDVI classes across the pre-fire, immediate post-fire, and recovery periods.

Table 4. Area and NDVI percentages.

NDVI	Pre-Fire (5/01/2024)	Post-Fire (25/01/2024)	Recovery (5/01/2026)
Low (≤0.2)	-/-	94.9 Ha (54.2%)	2.3 Ha (1.3%)
Moderate (0.2–0.5)	8.6 Ha (4.9%)	54.8 Ha (31.4%)	172.7 Ha (98.7%)
High (>0.5)	166.4 Ha (95.1%)	25.3 Ha (14.4%)	-/-
TOTAL	175 Ha (100%)	175 Ha (100%)	175 Ha (100%)

Table 5. Mean NDVI values (±SD) for the pre-fire, immediate post-fire, and recovery periods.

Metric	Pre-Fire (05-01-2024)	Post-Fire (25-01-2024)	Recovery (05-01-2026)
Mean NDVI	0.62	0.28	0.38
Standard Deviation	±0.09	±0.13	±0.06

Mean NDVI increased significantly between the immediate post-fire and 2026 recovery periods but remained below the pre-fire baseline (**Table 5**; paired *t*-test, $p < 0.001$). This result supports spectral greening but does not by itself demonstrate structural or functional ecosystem recovery.

4. Limitations

Several limitations should be considered. First, NDVI is a proxy for vegetation greenness and photosynthetic activity; it can saturate in dense canopies and may respond to understory growth without reflecting tree-canopy recovery. Second, the two-year post-fire period is short relative to forest recovery times. Third, no independent ecological ground-truth plots were available. The UAV assessment was based on visual interpretation of RGB orthophotos and cannot validate tree mortality, soil burn severity, species composition, seed-bank viability, or seedling recruitment. Fourth, the 500 validation checkpoints were purely random rather than stratified by severity, so rare classes may be underrepresented. Fifth, the UAV carried only an RGB sensor; multispectral or LiDAR measurements would permit stronger cross-scale validation. Finally, the analysis represents one fire event, limiting transferability to other vegetation, fuel, weather, and topographic conditions[28].

5. Discussion

The spectral and UAV products provide evidence of biophysical change, including canopy-surface loss, visible charring, and reduced greenness. They do not directly measure seed-bank viability, species turnover, succession, or ecosystem functioning. Any discussion of these processes is therefore framed as a hypothesis requiring field evaluation. The 175-ha burned area, located 1.1 km from Pamplona's urban perimeter, illustrates the exposure of Andean peri-urban landscapes to climate variability and anthropogenic fire pressure[6,7].

The dNBR classification placed 61.9% of the area in the moderate-high or high severity classes. This pattern differs from lower-severity distributions reported in some other environments[10,13] but is consistent with the strong influence of drought, terrain, land use, and pre-fire fuels on mapped severity[31]. Because the present study did not measure those drivers directly, their role in Fontibón should be interpreted as plausible rather than causal.

High and moderate-high dNBR patches may experience slower recovery. It is plausible that intense burning affected propagule availability and altered regeneration pathways, but seed-bank viability and species responses were not measured [32]. Low-severity and unburned patches may function as refugia, although this hypothesis requires field measurements of seed rain, germination, and seedling establishment. Fire-related changes in plant-soil water relations also depend on severity and ecosystem type [33]. Consequently, the restoration actions proposed here should be treated as spatial priorities for field verification rather than confirmed ecological diagnoses [18,34].

The NDVI series showed an immediate decline followed by widespread greening by 2026. Nevertheless, no area returned to the pre-fire high-NDVI class. This pattern is consistent with early foliage or herbaceous recovery while longer-lived structural components remain altered.

Large-scale evidence indicates that higher fire severity can prolong forest recovery [35]. Optical greenness indices may recover faster than woody biomass-sensitive signals, particularly in dense forests [36], and recent image-analysis methods also distinguish vegetation change from longer-term recovery [37]. Accordingly, the Fontibón NDVI trend should be interpreted as spectral greening rather than proof of ecological recovery. Future monitoring should combine NDVI with canopy-height, biomass, and field-composition measurements.

A principal strength of the study is its multiscale design. Sentinel-2 provided complete spatial coverage of the 175-ha area, while UAV products supplied sub-decimetric visual detail in heterogeneous patches. Similar work supports the use of UAV imagery as a high-resolution complement to satellite burn-severity mapping [17,19].

UAV orthophotos and 3D products supported delineation of the fire perimeter, identification of unburned patches, and visualization of heterogeneity not resolved within Sentinel-2 pixels. Comparable satellite analyses show the value of multitemporal imagery for reconstructing burn severity and progression [38]. Google Earth Engine improved reproducibility by supporting scripted filtering, cloud masking, compositing, and index calculation.

The present workflow primarily performs cross-scale comparison rather than full quantitative fusion of UAV and Sentinel-2 measurements. Future work should evaluate object-based image analysis, pixel-level fusion, and machine-learning models that jointly use spectral, textural, and structural features [23–25]. These approaches may reduce mixed-pixel effects and improve class-specific validation.

The severity map provides a spatial basis for prioritizing field assessment and restoration. High and moderate-high areas can be screened first for erosion control and assisted regeneration, whereas low-severity and unburned patches can be evaluated for passive restoration. These are management recommendations inferred from mapped severity, not verified ecological outcomes. Integration with local risk-management systems could improve preparedness and resource allocation [19,39].

As summarized in **Table 5**, mean NDVI increased significantly after the immediate post-fire period but remained below the pre-fire baseline. This trend supports continued monitoring and should not be interpreted as full structural recovery.

The main uncertainty sources were considered following Chuvieco et al. [11]:

1. Atmospheric effects: Sentinel-2 surface reflectance was atmospherically corrected with Sen2Cor. Residual aerosol and haze effects may still influence NBR; no independent atmospheric validation was available for this study.
2. Geometric registration: UAV orthophotos were co-registered to the Sentinel-2 grid with an RMSE of 0.5 pixels (5 m). Residual misregistration can affect comparisons along patch boundaries.
3. Cloud masking: QA60 filtering removed pixels identified as cloud-contaminated. Persistent fog reduced the availability of clear observations, and median compositing was used to limit this effect.
4. Classification uncertainty: comparison of dNBR classes with 500 UAV-interpreted checkpoints yielded 87.4% overall agreement (95% CI: 84.2–90.1%). Because the checkpoints were not stratified, class-specific estimates should be interpreted cautiously.
5. NDVI saturation: sensitivity to additional biomass decreases at high NDVI. This may compress pre-fire variability but does not alter the observation that 2026 values remained below the pre-fire high-NDVI class.

The results obtained support the planning of restoration processes, for which the following prioritization **Table 6** is proposed:

Table 6. Recovery prioritization scheme.

Severity Class	Area (ha)	Priority	Active Intervention	Timeline	Estimated Cost (USD/ha)
High (>0.66)	45.56	Critical	Mulching, check dams, native tree planting (Escallonia, Miconia), grazing exclusion	Years 1–5	$2,500–3,500
Moderate-High (0.44–0.66)	62.55	High	Assisted natural regeneration, seed broadcasting, erosion barriers	Years 1–3	$1,200–1,800
Moderate-Low (0.27–0.44)	32.54	Medium	Passive restoration + invasive species control	Years 1–2	$300–500
Low (0.10–0.27)	21.68	Low	Monitoring only	Ongoing	$50–100
Unburned	12.32	None	Conservation	—	$0

6. Conclusions

This study demonstrates an integrated workflow using UAV photogrammetry, Sentinel-2 imagery, and Google Earth Engine for post-fire assessment in a tropical mountain setting.

UAV imagery processed in Agisoft Metashape delineated a 175-ha affected area located 1.1 km from Pamplona. The UAV products complemented satellite observations where terrain complexity and cloud cover constrained conventional assessment, but they did not replace ecological field validation.

Sentinel-2 dNBR placed 61.9% of the area in moderate-high or high severity classes. These classes identify priority zones for field inspection and potential active restoration; they should not be interpreted as direct evidence of seed-bank loss, species replacement, or ecosystem-function decline.

NDVI showed widespread greening by January 2026, but no area returned to the pre-fire high-NDVI class. Longer monitoring with structural and ecological measurements is required to determine whether this spectral response develops into sustained ecosystem recovery.

The principal contribution is a replicable multiscale workflow for data-constrained mountain environments. Future work should incorporate stratified field sampling and quantitative fusion of UAV and satellite data.

The resulting maps can guide field verification, erosion-control planning, assisted regeneration, and protection of low-severity refugia. Final intervention decisions should integrate local ecological surveys, land-use conditions, feasibility, and community priorities.

The workflow may be transferable to other tropical mountain regions with steep slopes, persistent cloud cover, and ENSO-related drought. Transfer requires:

- Local validation of dNBR thresholds for the dominant vegetation types;
- Adaptation of UAV flight parameters to local terrain and airspace regulations; and
- Calibration of recovery trajectories using local field measurements.

Multi-fire studies across the Andes are needed to establish generalized severity thresholds and recovery curves. The contribution of this study is methodological rather than evidence of broad ecological generalizability.

Open-access Sentinel-2 data and Google Earth Engine, combined with commercial UAVs, can facilitate technology transfer to environmental and risk-management agencies operating under limited budgets.

Author Contributions

Conceptualization: C.E.O.-V., J.Y.V.-V., V.H.-C. and Y.A.G.-G.; methodology: C.E.O.-V., J.Y.V.-V., V.H.-C. and Y.A.G.-G.; software: C.E.O.-V., J.Y.V.-V. and V.H.-C.; validation: W.V.A., S.D.P., K.F.M. and A.M.J.C.G.; formal analysis: C.E.O.-V., J.Y.V.-V., V.H.-C. and Y.A.G.-G.; investigation: C.E.O.-V. and J.Y.V.-V.; resources: W.V.A., S.D.P., K.F.M. and A.M.J.C.G.; data curation: C.E.O.-V. and J.Y.V.-V.; writing—original draft: Y.A.G.-G.; writing—review and editing: Y.A.G.-G.; visualization: C.E.O.-V. and J.Y.V.-V.; supervision: V.H.-C., W.V.A., S.D.P. and K.F.M.; project administration: C.E.O.-V. and J.Y.V.-V.; funding acquisition: C.E.O.-V. and J.Y.V.-V. All authors have read and agreed to the published version of the manuscript.

Funding

This research received no external funding.

Institutional Review Board Statement

Not applicable.

Informed Consent Statement

Not applicable.

Data Availability Statement

No new data were generated in this study. The datasets used and/or analyzed during the current research are not publicly available due to confidentiality and embargo restrictions but may be made available from the corresponding authors upon reasonable and justified request.

Conflicts of Interest

The authors declare no conflict of interest.

AI Use Statement

During the preparation of this manuscript, the authors used Grammarly and DeepL.com solely for language refinement. No AI tools were used for data analysis, interpretation, or generation of scientific content. All outputs were critically reviewed and edited by the authors. The authors take full responsibility for the integrity and accuracy of the work.

References

[1] Pausas, J.G., Keeley, J.E., 2019. Wildfires as an ecosystem service. Frontiers in Ecology and the Environment. 17(5), 289–295. DOI: https://doi.org/10.1002/fee.2044

[2] Certini, G., 2005. Effects of fire on properties of forest soils: A review. Oecologia. 143(1), 1–10. DOI: https://doi.org/10.1007/s00442-004-1788-8

[3] Mataix-Solera, J., Cerdà, A., Arcenegui, V., et al., 2011. Fire effects on soil aggregation: A review. Earth-Science Reviews. 109(1–2), 44–60. DOI: https://doi.org/10.1016/j.earscirev.2011.08.002

[4] van der Werf, G.R., Randerson, J.T., Giglio, L., et al., 2017. Global fire emissions estimates during 1997–2016. Earth System Science Data. 9(2), 697–720. DOI: https://doi.org/10.5194/essd-9-697-2017

[5] Doerr, S.H., Santín, C., 2016. Global trends in wildfire and its impacts: Perceptions versus realities in a changing world. Philosophical Transactions of the Royal Society B: Biological Sciences. 371(1696), 20150345. DOI: https://doi.org/10.1098/rstb.2015.0345

[6] Poveda, G., Salas, H.D., Mesa, Ó.J., et al., 2020. Generalized synchronization between ENSO and hydrological variables in Colombia: A recurrence quantification approach. Frontiers in Applied Mathematics and Statistics. 6, 3. DOI: https://doi.org/10.3389/fams.2020.00003

[7] Armenteras, D., González, T.M., Vargas, J.O., et al., 2020. Fire in the ecosystems of northern South America: Advances in the ecology of tropical fires in Colombia, Ecuador and Peru. Caldasia. 42(1), 1–16. DOI: https://doi.org/10.15446/caldasia.v42n1.77353 (in Spanish)

[8] Lentile, L.B., Holden, Z.A., Smith, A.M.S., et al., 2006. Remote sensing techniques to assess active fire characteristics and post-fire effects. International Journal of Wildland Fire. 15(3), 319–345. DOI: https://doi.org/10.1071/WF05097

[9] Parsons, A., Robichaud, P.R., Lewis, S.A., et al., 2010. Field Guide for Mapping Post-Fire Soil Burn Severity. Department of Agriculture: Fort Collins, CO, USA.

[10] Quintano, C., Fernández-Manso, A., Roberts, D.A., 2017. Burn severity mapping from Landsat MESMA fraction images and land surface temperature. Remote Sensing of Environment. 190, 83–95. DOI: https://doi.org/10.1016/j.rse.2016.12.009

[11] Chuvieco, E., Aguado, I., Salas, J., et al., 2020. Satellite remote sensing contributions to wildland fire science and management. Current Forestry Reports. 6(2), 81–96. DOI: https://doi.org/10.1007/s40725-020-00116-5

[12] Zhu, Z., Wulder, M.A., Roy, D.P., et al., 2019. Benefits of the free and open Landsat data policy. Remote Sensing of Environment. 224, 382–385. DOI: https://doi.org/10.1016/j.rse.2019.02.016

[13] Pérez-Cabello, F., Montorio, R., Alves, D.B., 2021. Remote sensing techniques to assess post-fire vegetation recovery. Current Opinion in Environmental Science & Health. 21, 100251. DOI: https://doi.org/10.1016/j.coesh.2021.100251

[14] Eidenshink, J., Schwind, B., Brewer, K., et al., 2007. A project for monitoring trends in burn severity. Fire Ecology. 3(1), 3–21. DOI: https://doi.org/10.4996/fireecology.0301003

[15] Key, C.H., Benson, N.C., 2006. Landscape assessment: Sampling and analysis methods. In: Lutes, D.C., Keane, R.E., Caratti, J.F., et al. (Eds.). FIREMON: Fire Effects Monitoring and Inventory System. Department of Agriculture: Fort Collins, CO, USA.

[16] Parks, S.A., Dillon, G.K., Miller, C., 2014. A new metric for quantifying burn severity: the relativized burn ratio. Remote Sensing. 6(3), 1827–1844. DOI: https://doi.org/10.3390/rs6031827

[17] Simes, T., Pádua, L., Moutinho, A., 2024. Wildfire burnt area severity classification from UAV-based RGB and multispectral imagery. Remote Sensing. 16(1), 30. DOI: https://doi.org/10.3390/rs16010030

[18] Robichaud, P.R., Lewis, S.A., Laes, D.Y.M., et al., 2007. Postfire soil burn severity mapping with hyperspectral image unmixing. Remote Sensing of Environ-

ment. 108(4), 467–480. DOI: https://doi.org/10.1016/j.rse.2006.11.027

[19] Guiop-Servan, R.E., Cotrina-Sanchez, A., Puerta-Culqui, J., et al., 2025. Remote sensing for wildfire mapping: A comprehensive review of advances, platforms, and algorithms. Fire. 8(8), 316. DOI: https://doi.org/10.3390/fire8080316

[20] Hoyos, J.D., Suárez, G., Velásquez, J.D., et al., 2025. Complex remote sensing analysis of fire precursors in the tropical region: Case study. Forests. 16(5), 779. DOI: https://doi.org/10.3390/f16050779

[21] Morante-Carballo, F., Bravo-Montero, L., Carrión-Mero, P., et al., 2022. Forest fire assessment using remote sensing to support the development of an action plan proposal in Ecuador. Remote Sensing. 14(8), 1783. DOI: https://doi.org/10.3390/rs14081783

[22] Gao, B., Jia, W., Wang, Q., et al., 2025. All-weather forest fire automatic monitoring and early warning application based on multi-source remote sensing data: Case study of Yunnan. Fire. 8(9), 344. DOI: https://doi.org/10.3390/fire8090344

[23] Chen, X., Zhang, Y., Wang, S., et al., 2024. Comparative study of machine learning methods for mapping forest fire areas using Sentinel-1B and 2A imagery. Frontiers in Remote Sensing. 5, 1446641. DOI: https://doi.org/10.3389/frsen.2024.1446641

[24] Suwanprasit, C., Shahnawaz, 2024. Mapping burned areas in Thailand using Sentinel-2 imagery and OBIA techniques. Scientific Reports. 14, 9609. DOI: https://doi.org/10.1038/s41598-024-60512-w

[25] Lee, S.H., Lee, M.H., Kang, T.H., et al., 2025. Comparative analysis of dNBR, dNDVI, SVM kernels, and ISODATA for wildfire-burned area mapping using Sentinel-2 imagery. Remote Sensing. 17(13), 2196. DOI: https://doi.org/10.3390/rs17132196

[26] El Khatib, D., Kallas, G., Bechara, J., et al., 2026. Digital landscapes: assessing fire severity and its drivers using remote sensing and Google Earth Engine based on dNBR and NPP indicators. Remote Sensing. 18(10), 1654. DOI: https://doi.org/10.3390/rs18101654

[27] Quintero, N., Viedma, O., Urbieta, I.R., et al., 2019. Assessing landscape fire hazard by multitemporal automatic classification of Landsat time series using Google Earth Engine in west-central Spain. Forests. 10(6), 518. DOI: https://doi.org/10.3390/f10060518

[28] Llorens, R., Sobrino, J.A., Fernández, C., et al., 2024. Soil burn severity assessment using Sentinel-2 and radiometric measurements. Fire. 7(12), 487. DOI: https://doi.org/10.3390/fire7120487

[29] Epting, J., Verbyla, D., Sorbel, B., 2005. Evaluation of remotely sensed indices for assessing burn severity in interior Alaska using Landsat TM and ETM+. Remote Sensing of Environment. 96(3–4), 328–339. DOI: https://doi.org/10.1016/j.rse.2005.03.002

[30] Drusch, M., Del Bello, U., Carlier, S., et al., 2012. Sentinel-2: ESA's optical high-resolution mission for GMES operational services. Remote Sensing of Environment. 120, 25–36. DOI: https://doi.org/10.1016/j.rse.2011.11.026

[31] Castro-Melgar, I., Tsagkou, A., Zacharopoulou, M., et al., 2025. Wildfires during early summer in Greece (2024): Burn severity and land use dynamics through Sentinel-2 data. Forests. 16(2), 268. DOI: https://doi.org/10.3390/f16020268

[32] Moreira, F., Ascoli, D., Safford, H., et al., 2020. Wildfire management in Mediterranean-type regions: Paradigm change needed. Environmental Research Letters. 15(1), 011001. DOI: https://doi.org/10.1088/1748-9326/ab541e

[33] Baur, M.J., Friend, A.D., Pellegrini, A.F.A., 2024. Widespread and systematic effects of fire on plant-soil water relations. Nature Geoscience. 17(11), 1115–1120. DOI: https://doi.org/10.1038/s41561-024-01563-6

[34] Bodí, M.B., Mataix-Solera, J., Doerr, S.H., et al., 2011. The wettability of ash from burned vegetation and its relationship to Mediterranean plant species type, burn severity and total organic carbon content. Geoderma. 160(3–4), 599–607.

[35] Lv, Q., Chen, Z., Wu, C., et al., 2025. Increasing severity of large-scale fires prolongs recovery time of forests globally since 2001. Nature Ecology & Evolution. 9, 980–992. DOI: https://doi.org/10.1038/s41559-025-02683-x

[36] Bousquet, E., Mialon, A., Rodriguez-Fernandez, N., et al., 2022. Monitoring post-fire recovery of various vegetation biomes using multi-wavelength satellite remote sensing. Biogeosciences. 19, 3317–3336. DOI: https://doi.org/10.5194/bg-19-3317-2022

[37] Priya, R.S., Vani, K., 2024. Vegetation change detection and recovery assessment based on post-fire satellite imagery using deep learning. Scientific Reports. 14, 12611. DOI: https://doi.org/10.1038/s41598-024-63047-2

[38] Oseghae, I., Bhaganagar, K., Mestas-Nuñez, A.M., 2024. The Dolan Fire of central coastal California: burn severity and progression using satellite observations. Remote Sensing. 16(10), 1693. DOI: https://doi.org/10.3390/rs16101693

[39] San-Miguel-Ayanz, J., Durrant, T., Boca, R., et al., 2020. Forest Fires in Europe, Middle East and North Africa 2019. Publications Office of the European Union: Luxembourg City, Luxembourg.